

Special functions in phase space: Mathieu functions

This article has been downloaded from IOPscience. Please scroll down to see the full text article.

1998 J. Phys. A: Math. Gen. 31 6725

(<http://iopscience.iop.org/0305-4470/31/31/017>)

View [the table of contents for this issue](#), or go to the [journal homepage](#) for more

Download details:

IP Address: 171.66.16.102

The article was downloaded on 02/06/2010 at 07:09

Please note that [terms and conditions apply](#).

Special functions in phase space: Mathieu functions

Go Torres-Vega[†] J D Morales-Guzmán[‡] and A Zúñiga-Segundo[§]

[†] Departamento de Física, Centro de Investigación y de Estudios Avanzados del IPN, Apartado Postal 14-740, 07000 México, DF, Mexico

[‡] División de Ciencias Básicas e Ingeniería, Área de Física, Universidad Autónoma Metropolitana, Unidad Azcapotzalco, Av. San Pablo Núm. 180, 02200 México, DF, Mexico

[§] Departamento de Física, Escuela Superior de Física y Matemáticas del IPN, Edificio 9, Unidad Profesional ‘Adolfo López Mateos’, 07738 México, DF, Mexico

Received 8 May 1998

Abstract. We introduce functions which are solutions to a coherent-state representation of the Schrödinger equation for the pendulum potential. These functions are interpolation functions between the coordinate and momentum solutions for the quantum pendulum. We also introduce their classical analogues which are stationary solutions to the classical Liouville equation.

1. Introduction

For the free particle, the linear potential and the harmonic oscillator, the coherent-state representation has led to phase-space functions which are solutions to equations which resemble a Schrödinger equation in phase space. These functions were found to comply with the uncertainty relationship and they were also found to approach a classical stationary density in the appropriate limit [1–11]. Even though the introduction of an additional variable in the coordinate representation of quantum mechanics, in a more or less arbitrary manner, makes things more complicated, by using coherent-states as a basis for a ‘phase-space’ wavefunction we are led to probability densities which contain quantum information and that can be used in making comparisons between classical and quantum dynamics.

In this paper, we introduce phase-space functions which can be used as eigenfunctions for the quantum pendulum in phase space. In section 2, we briefly review the coherent-state representation as is used in this work. The set of functions used to solve the quantum pendulum model in phase space is discussed in section 4. These functions are phase-space versions of the Mathieu functions used in coordinate space. In section 3, we use these functions to solve a Schrödinger-like equation for the quantum pendulum in phase space. We analyse these functions for the cases in which the quantum number is small or large and we also look for what the classical limit of them could be.

2. Coherent-state quantum phase-space representation

In this paper, we make use of a coherent-state representation of non-relativistic quantum mechanics [1–11] in which the operators associated to momentum \hat{P} , coordinate \hat{Q} , and inverse coordinate \hat{Q}^{-1} , are given by

$$\hat{P} \leftrightarrow \frac{p}{2} - i\hbar \frac{\partial}{\partial q} \quad \hat{Q} \leftrightarrow \frac{q}{2} + i\hbar \frac{\partial}{\partial p} \quad \text{and} \quad \hat{Q}^{-1} \leftrightarrow -\frac{i}{\hbar} e^{ipq/2\hbar} \int dp e^{-ipq/2\hbar}. \quad (1)$$

They are just half-Bopp operators. [2] These operators do not commute with each other, in fact $[\hat{Q}, \hat{P}] = i\hbar$. Based on these operators, the phase-space Schrödinger equation is given by

$$i\hbar \frac{\partial}{\partial t} \langle \Gamma | \psi \rangle = \left[\frac{1}{2m} \left(\frac{p}{2} - i\hbar \frac{\partial}{\partial q} \right)^2 + V \left(\frac{q}{2} + i\hbar \frac{\partial}{\partial p} \right) \right] \langle \Gamma | \psi \rangle \quad (2)$$

where $\langle \Gamma | \psi \rangle = \psi(\Gamma; t)$ denotes the time-dependent phase-space function. Within this representation one can analyse formally, as well as numerically, quantum dynamics entirely in phase space in the same way as is done in coordinate or abstract representations.

For instance, the finding of eigenvalues and eigenfunctions of the Hamiltonian operator can be done by analytically solving the eigenvalue problem,

$$\left[\frac{1}{2m} \left(\frac{p}{2} - i\hbar \frac{\partial}{\partial q} \right)^2 + V \left(\frac{q}{2} + i\hbar \frac{\partial}{\partial p} \right) \right] \langle \Gamma | \psi_E \rangle = E \langle \Gamma | \psi_E \rangle \quad (3)$$

as is done in the following section for the pendulum, or numerically, or by propagating a non-stationary initial phase-space function $\langle \Gamma | \psi_0 \rangle$ and utilizing the standard time-dependent formalism which requires use of the Fourier transform $\lim_{T \rightarrow \infty} \int_{-T}^T dt \exp(i\omega t) \langle \psi_0 | \psi_t \rangle$, from which the eigenvalues are obtained, and of

$$\langle \Gamma | \psi_E \rangle \propto \lim_{T \rightarrow \infty} \frac{1}{2T} \int_{-T}^T dt e^{iEt/\hbar} \langle \Gamma | \psi_t \rangle \quad (4)$$

which gives the eigenfunctions.

Another way of relating coordinate or momentum spaces with this phase-space representation is by means of unitary operators as

$$\begin{aligned} \exp \left(-i\hbar \frac{\partial}{\partial p} \frac{\partial}{\partial q} \right) e^{ipq/2\hbar} \left[\frac{1}{2m} \left(\frac{p}{2} - i\hbar \frac{\partial}{\partial q} \right)^2 + V \left(\frac{q}{2} + i\hbar \frac{\partial}{\partial p} \right) \right] e^{-ipq/2\hbar} \exp \left(i\hbar \frac{\partial}{\partial p} \frac{\partial}{\partial q} \right) \\ = \frac{1}{2m} \left(-i\hbar \frac{\partial}{\partial q} \right)^2 + V(q) \end{aligned} \quad (5)$$

and

$$\begin{aligned} \exp \left(i\hbar \frac{\partial}{\partial p} \frac{\partial}{\partial q} \right) e^{-ipq/2\hbar} \left[\frac{1}{2m} \left(\frac{p}{2} - i\hbar \frac{\partial}{\partial q} \right)^2 + V \left(\frac{q}{2} + i\hbar \frac{\partial}{\partial p} \right) \right] e^{ipq/2\hbar} \exp \left(-i\hbar \frac{\partial}{\partial p} \frac{\partial}{\partial q} \right) \\ = \frac{p^2}{2m} + V \left(i\hbar \frac{\partial}{\partial p} \right). \end{aligned} \quad (6)$$

These results indicate that the eigenvalues are the same for all three representations, coordinate, momentum and phase space. We also see that, when the phase-space equation is reduced to the coordinate equation in the above manner, the momentum variable results in a superconservative variable which does not participate in the dynamics, and something similar happens when we reduce the phase-space equation to the momentum one.

3. Quantum pendulum in phase space

The classical Hamiltonian for the pendulum is given by [13]

$$H(\theta, L) = \frac{L^2}{8ml^2} + mgl(1 - \cos 2\theta) \quad (7)$$

where L is the momentum conjugate to the angle variable θ , m is the mass of the particle, g is the acceleration due to gravity and l is the length of the pendulum. Since this system is a conservative one, the energy E is constant and equal to the Hamiltonian $E = H(\theta, L)$. Even though the space considered in section 2 is a $R \times R$ phase space and the pendulum space is a $S \times Z$ phase space, we will follow the quantization rule of replacing conjugate variables with the phase-space operators of section 2, in a similar way as is done in coordinate representation. Then, the quantization of the classical pendulum is made by means of the replacements

$$E \rightarrow i\hbar \frac{\partial}{\partial t} \quad L \rightarrow \frac{L}{2} - i\hbar \frac{\partial}{\partial \theta} \quad \theta \rightarrow \frac{\theta}{2} + i\hbar \frac{\partial}{\partial L} \quad (8)$$

which lead to the phase-space Schrödinger-like equation

$$i\hbar \frac{\partial}{\partial t} \psi(\theta, L; t) = \left\{ \frac{1}{8ml^2} \left(\frac{L}{2} - i\hbar \frac{\partial}{\partial \theta} \right)^2 + mgl \left\{ 1 - \cos \left[2 \left(\frac{\theta}{2} + i\hbar \frac{\partial}{\partial L} \right) \right] \right\} \right\} \psi(\theta, L; t). \quad (9)$$

The scaling of the angular momentum L by \hbar and the rearranging of terms gives, for the time-independent equation,

$$\left\{ \left(\frac{\bar{L}}{2} - i \frac{\partial}{\partial \theta} \right)^2 - a + 2q \cos \left[2 \left(\frac{\theta}{2} + i \frac{\partial}{\partial \bar{L}} \right) \right] \right\} \psi(\theta, \bar{L}) = 0 \quad (10)$$

where

$$\bar{L} = \frac{L}{\hbar} \quad a = 8 \frac{ml^2}{\hbar^2} (E - mgl) \quad q = -\frac{4m^2 g l^3}{\hbar^2}. \quad (11)$$

This equation has the form of a Mathieu equation but in phase space. Equation (13) (see the appendix), has an infinite number of solutions in phase space, namely $\text{cep}_n(\theta, L, q)$ and $\text{sep}_n(\theta, L, q)$. These functions are interpolation functions between the eigenfunctions in coordinate and momentum spaces depending upon the value of the parameter $0 < \sigma < \infty$.

A density plot of the squared magnitude of the lowest five eigenfunctions, and one with large energy, with $q = -1$ and $\sigma = 1/\sqrt{2}$, are shown in figure 1. They are ordered according to increasing values of energy (values of a), $a = -0.4543, -0.1102, 2.1411, 3.9170, 4.3704$ and 156.253221 . We have chosen $\sigma = 1/\sqrt{2}$ because this is the value which leads to densities that better resemble their classical analogues and give equal weight to both θ and L (see the appendix).

In the four lowest eigenfunctions, quantum interference is so strong that the density does not follow a classical trajectory, but for large energies the quantum density resembles the classical trajectory. The value of a closest to the energy of the separatrix is 2.1411 which corresponds to sep_1 . For this function, the maximum probability is at the crossing point of the separatrix, the hyperbolic points at $p = 0$ and $\theta = (2n + 1)\pi$.

In figure 1 the heights of the contour lines are equally spaced and the height of the lowest contour level is at 0.1 of the maximum height of the density. However, the part of the density with very small values gives additional information about the quantum dynamics. In figure 2 we show the same eigenfunctions as in figure 1 but now the heights of the contour levels increase as z^8 , with the lowest level at 10^{-8} of the maximum value. We can see that there is a small part of the density that exists far from where the density is a maximum, in regions of large classical energy. The number of zeros goes from 16 to 24 in a period of 2π in θ and their distribution in phase space varies with the eigenfunction.

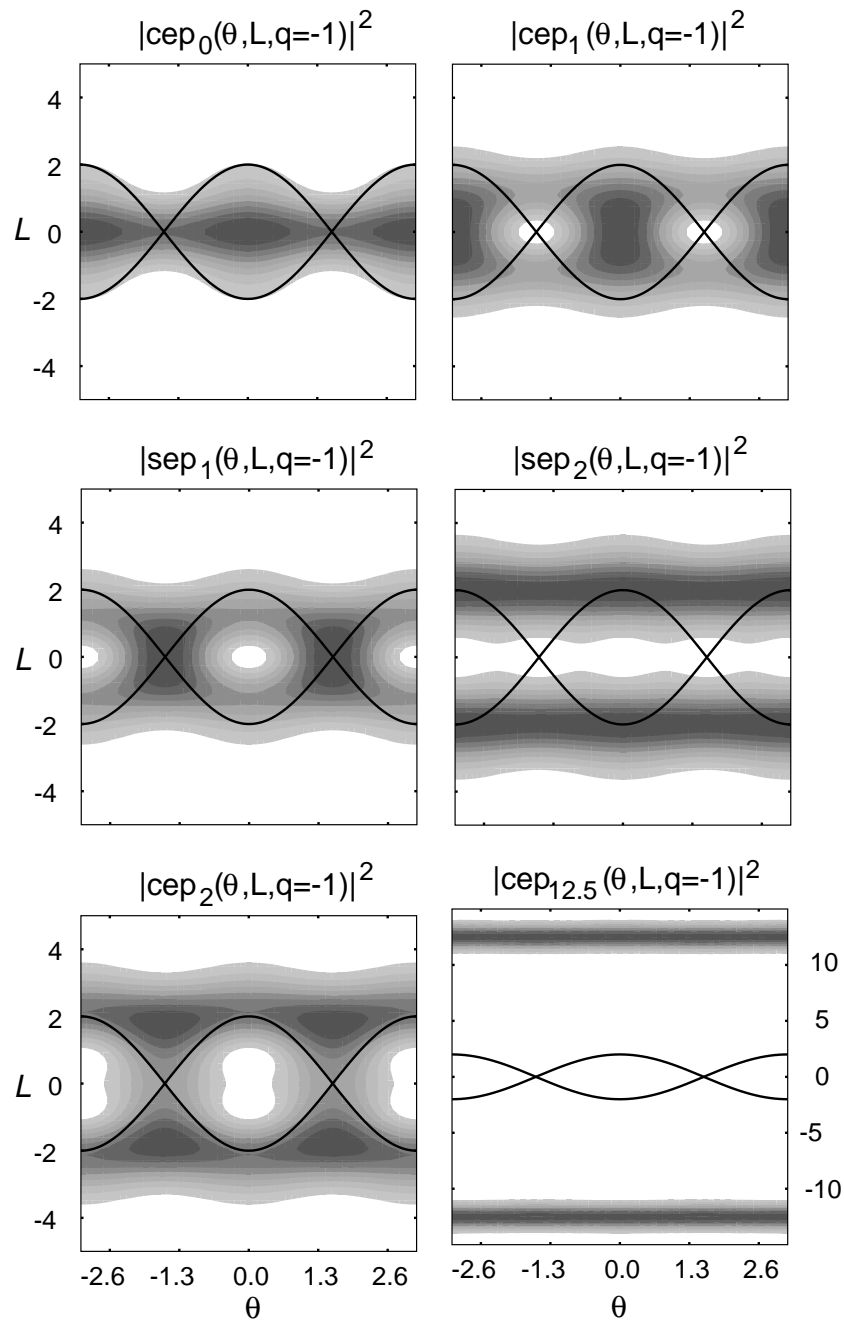


Figure 1. Density plots of some pendulum eigenfunctions in phase space. The values of a are -0.4543 , -0.1102 , 2.1411 , 3.9170 , 4.3704 and 156.253221 . The lines in these plots indicate the separatrix for this system.

We expect that the quantum densities approach the classical ones when $\hbar \rightarrow 0$ or when the energy is large, i.e. when a is large. Due to the rescaling we made, the limit $\hbar \rightarrow 0$ is

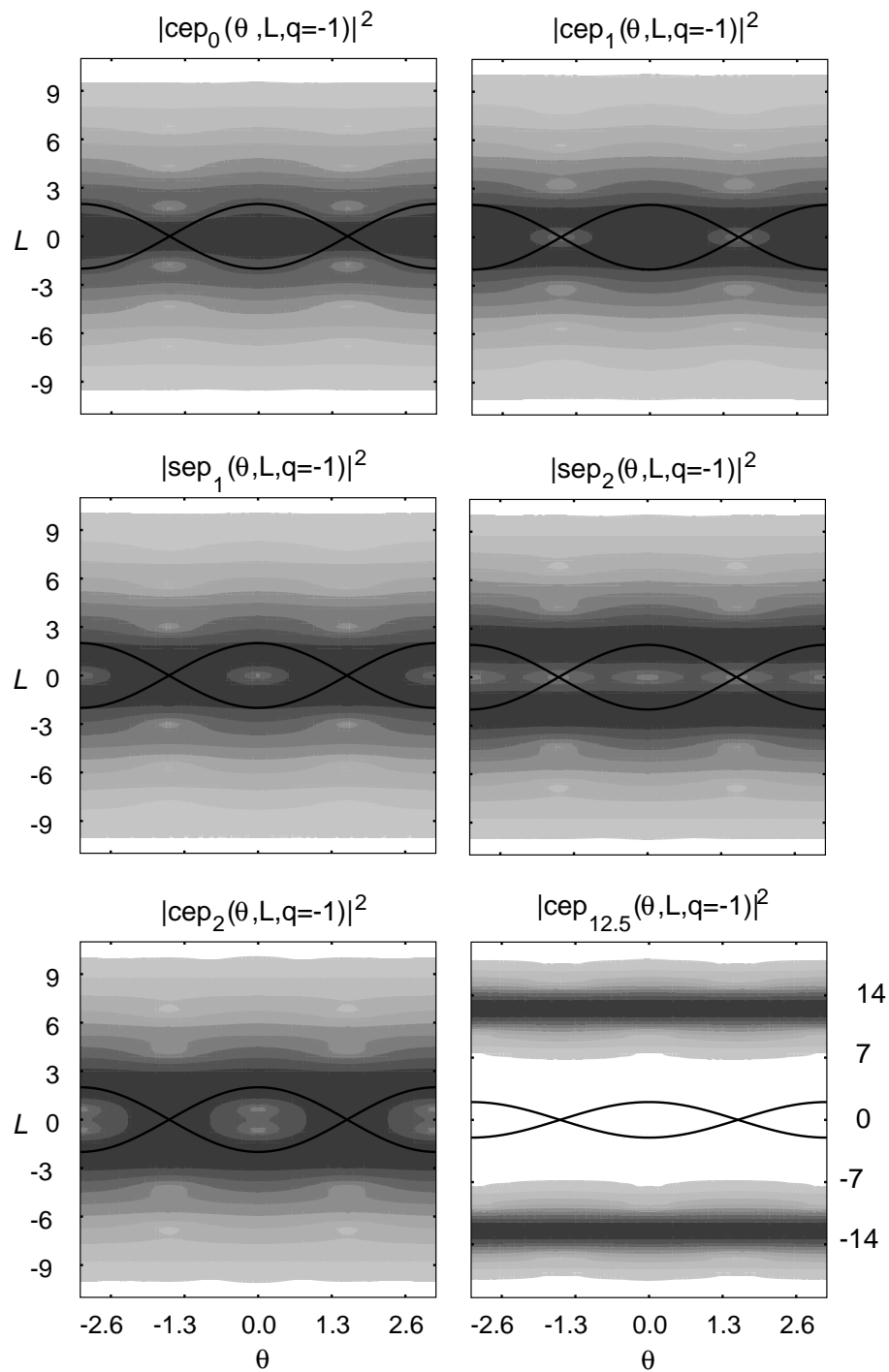


Figure 2. Density plots of the same pendulum eigenfunctions in phase space as in figure 1, but now the heights of the contour levels increase as z^8 .

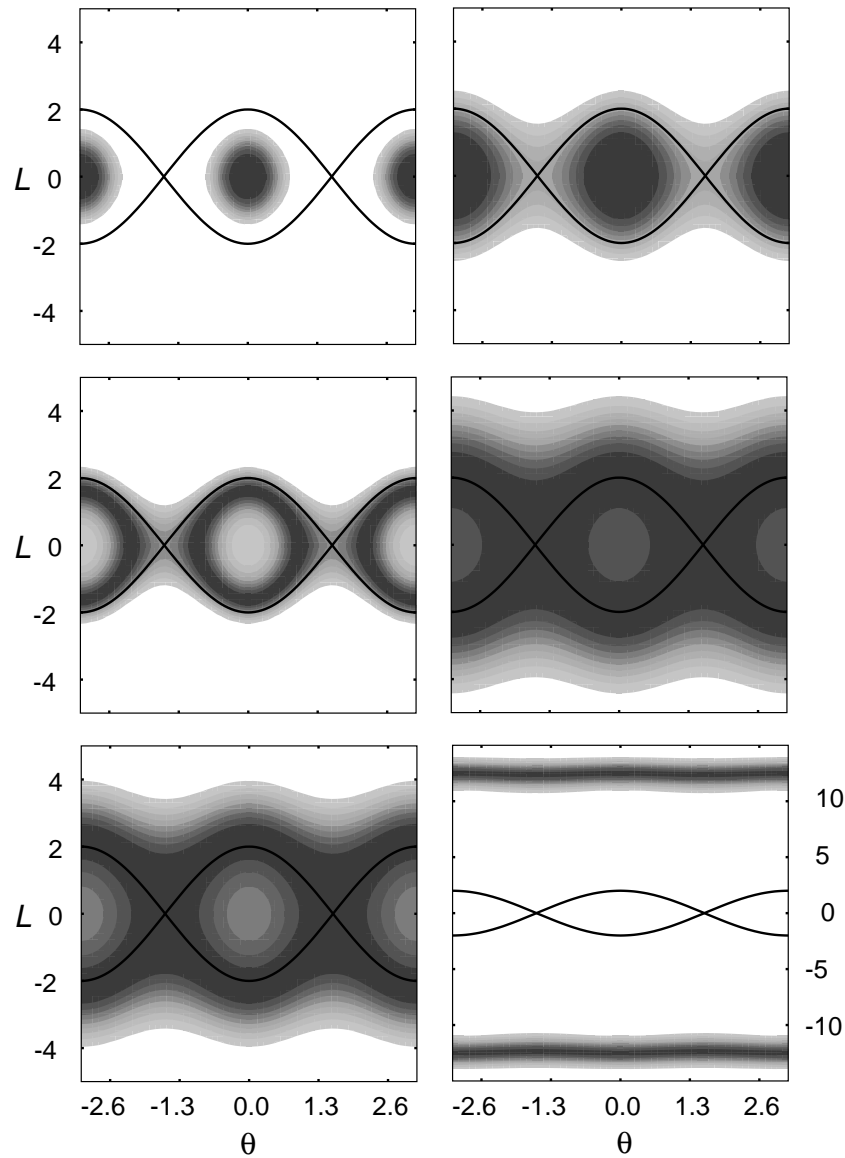


Figure 3. Density plots of the classical analogues, $\exp[-(a - H)^2/2\lambda^2 a^2]$, corresponding to the quantum densities in figure 1. The values of σ are 3, 20, 0.6, 0.6, 0.65, 0.5, 0.45 and 0.4. The lines indicate the separatrix for this system.

equivalent to large values of a and q . The classical analogues taken here are

$$e^{-[a - H(\theta, L)]^2/2\lambda^2} \quad (12)$$

where the dimensionless parameter λ has been chosen as to obtain a classical density with the same width in p as the quantum one. In figure 3 there are density plots of this classical density for the same energy values (i.e. the same values of a) as those in figure 1 decreased by the ground value.

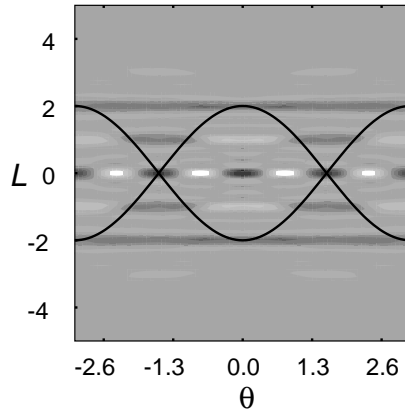


Figure 4. Density plot of the Wigner density for the pendulum ground state.

After a comparison between the densities in figures 1 and 3, we see that at low energies, there are big differences between quantum and classical densities, but for large energies the two densities are very similar.

4. Concluding remarks

The phase-space analysis of quantum systems is an intriguing and interesting subject. In this work, we have illustrated one way of doing phase-space quantization with the quantization of the pendulum model. The proposed functions are the solutions to a time-independent Schrödinger-like equation in phase space, which comply with the uncertainty relationship, and, depending on the value of the parameter σ , they can be used to describe the quantum system in coordinate, momentum or phase spaces. These functions approach a classical stationary density in the limit of large energies.

We can compare with another of the phase-space densities, namely the Wigner function. For instance, the Wigner density corresponding to the pendulum ground state is shown in figure 4. As usual, the Wigner function is not large around classical trajectories and oscillates on other regions of phase space.

With the results in this paper, we have increased the collection of special functions and eigenstates in phase space which can be used in the comparison between quantum and classical dynamics. The use of a coherent-state representation can be a good option for the analysis of quantum systems in phase space.

We have used this representation in the analysis of quantum dynamics around separatrices and stochastic webs in regular and non-regular systems [14].

Acknowledgments

We are very grateful for financial support to CONACyT and SNI, México.

Appendix. Mathieu functions in phase space

Let us consider the two-variables equation

$$\left\{ \left(\frac{L}{2} - i \frac{\partial}{\partial \theta} \right)^2 - a + 2q \cos \left[2 \left(\frac{\theta}{2} + i \frac{\partial}{\partial L} \right) \right] \right\} w(\theta, L) = 0. \quad (13)$$

A solution to the above equation is written in terms of a set of eigenfunctions of the operator $(L/2 - i\partial/\partial\theta)^2$,

$$\text{cosp}(\theta, L, m) = \sqrt{2\sigma\sqrt{2\pi}} \exp\left[-\frac{iL}{2}(\theta - i2\sigma^2 L) - \sigma^2 m^2\right] \cos[m(\theta - i2\sigma^2 L)] \quad (14)$$

$$\text{sinp}(\theta, L, m) = \sqrt{2\sigma\sqrt{2\pi}} \exp\left[-\frac{iL}{2}(\theta - i2\sigma^2 L) - \sigma^2 m^2\right] \sin[m(\theta - i2\sigma^2 L)] \quad (15)$$

where $0 < \sigma < \infty$ is a real parameter which meaning is given below. These are the phase-space versions of $\cos(x)$ and $\sin(x)$ appropriate for a phase-space analysis of quantum systems. Some of the properties of these functions are

$$|\text{cosp}(\theta, L, m)|^2 = \sigma \sqrt{\frac{\pi}{2}} \left[e^{-2\sigma^2(m-L)^2} + e^{-2\sigma^2(m+L)^2} + 2e^{-\sigma^2[(m+L)^2 + (m-L)^2]} \cos(2m\theta) \right] \quad (16)$$

$$|\text{sinp}(\theta, L, m)|^2 = \sigma \sqrt{\frac{\pi}{2}} \left[e^{-2\sigma^2(m-L)^2} + e^{-2\sigma^2(m+L)^2} - 2e^{-\sigma^2[(m+L)^2 + (m-L)^2]} \cos(2m\theta) \right] \quad (17)$$

$$\left(\frac{L}{2} - i\frac{\partial}{\partial\theta}\right) \text{cosp}(\theta, L, m) = i m \text{sinp}(\theta, L, m) \quad (18)$$

$$\left(\frac{L}{2} - i\frac{\partial}{\partial\theta}\right) \text{sinp}(\theta, L, m) = -i m \text{cosp}(\theta, L, m) \quad (19)$$

$$\left(\frac{L}{2} - i\frac{\partial}{\partial\theta}\right)^2 \text{cosp}(\theta, L, m) = m^2 \text{cosp}(\theta, L, m) \quad (20)$$

$$\left(\frac{L}{2} - i\frac{\partial}{\partial\theta}\right)^2 \text{sinp}(\theta, L, m) = m^2 \text{sinp}(\theta, L, m) \quad (21)$$

$$\left(\frac{\theta}{2} + i\frac{\partial}{\partial L}\right) \text{cosp}(\theta, L, m) = (\theta - 2iL\sigma^2) \text{cosp}(\theta, L, m) - 2\sigma^2 m \text{sinp}(\theta, L, m) \quad (22)$$

$$\left(\frac{\theta}{2} + i\frac{\partial}{\partial L}\right) \text{sinp}(\theta, L, m) = (\theta - 2iL\sigma^2) \text{sinp}(\theta, L, m) + 2\sigma^2 m \text{cosp}(\theta, L, m) \quad (23)$$

$$\cos\left[2\left(\frac{\theta}{2} + i\frac{\partial}{\partial L}\right)\right] \text{cosp}(\theta, L, m) = \frac{1}{2} [\text{cosp}(\theta, L, m+2) + \text{cosp}(\theta, L, m-2)] \quad (24)$$

$$\cos\left[2\left(\frac{\theta}{2} + i\frac{\partial}{\partial L}\right)\right] \text{sinp}(\theta, L, m) = \frac{1}{2} [\text{sinp}(\theta, L, m+2) + \text{sinp}(\theta, L, m-2)]. \quad (25)$$

From these relations we can see that the modulus squared of these functions are periodic, of period π in θ , the peaks are located along the lines $L = \pm m$ and that they decay as the exponential of $(m \pm L)^2$ in the L direction. When $\sigma \rightarrow 0$, $|\text{cosp}(\theta, L, m)|^2 \rightarrow 2\sigma\sqrt{2\pi} \cos^2(m\theta)$ and $|\text{sinp}(\theta, L, m)|^2 \rightarrow 2\sigma\sqrt{2\pi} \sin^2(m\theta)$. However, when σ is large, they become $|\text{cosp}(\theta, L, m)|^2 = |\text{sinp}(\theta, L, m)|^2 \approx \pi[\delta(m-L) + \delta(m+L)]/2$. Thus, cosp and sinp are σ -dependent interpolation functions between these two limiting functions. Density plots of the real and imaginary parts of some of these functions can be found in figures 5 and 6.

The equalities

$$\left[\left(\frac{L}{2} - i\frac{\partial}{\partial\theta}\right) + \frac{i}{2\sigma^2} \left(\frac{\theta}{2} + i\frac{\partial}{\partial L}\right)\right] \text{cosp}(\theta, L, m) = \left(L + \frac{i\theta}{2\sigma^2}\right) \text{cosp}(\theta, L, m) \quad (26)$$

$$\left[\left(\frac{L}{2} - i\frac{\partial}{\partial\theta}\right) + \frac{i}{2\sigma^2} \left(\frac{\theta}{2} + i\frac{\partial}{\partial L}\right)\right] \text{sinp}(\theta, L, m) = \left(L + \frac{i\theta}{2\sigma^2}\right) \text{sinp}(\theta, L, m) \quad (27)$$

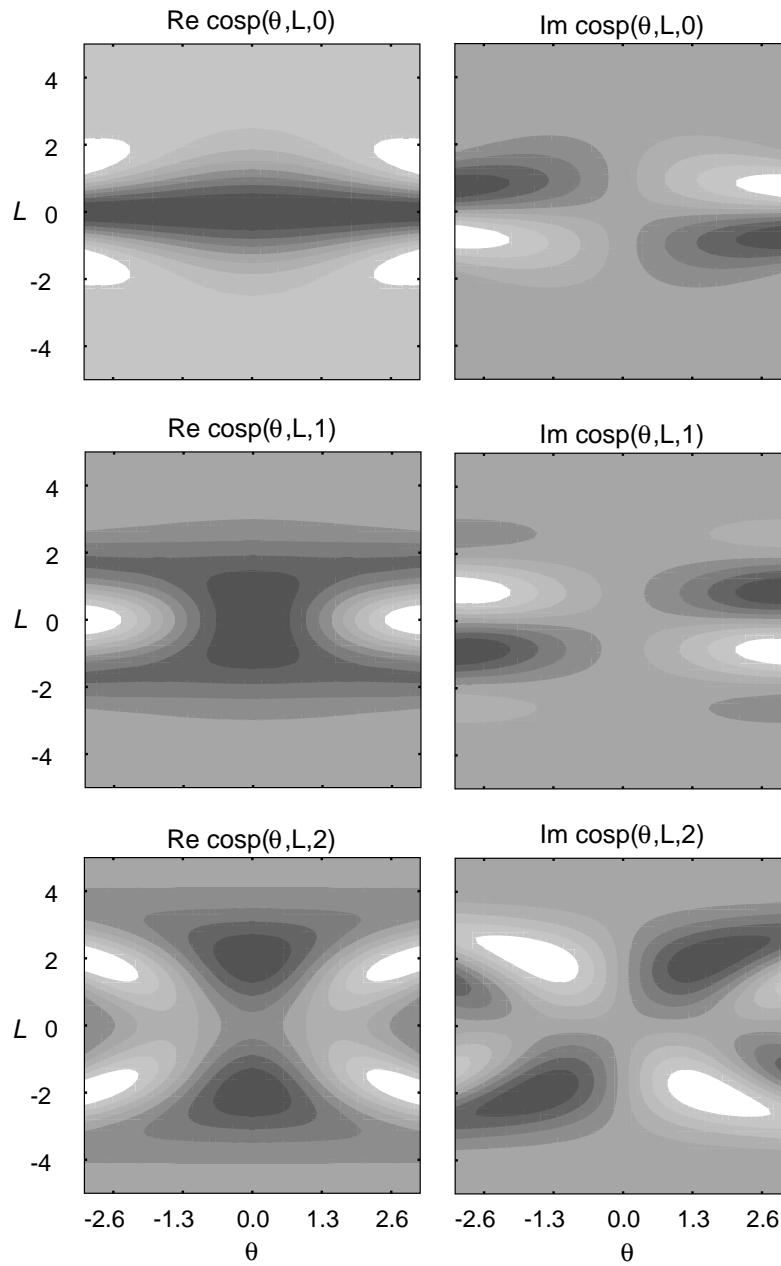


Figure 5. Density plots of the real and imaginary parts of $\text{cosp}(\theta, L, m)$ for $m = 0, 1, 2$ and $\sigma = 1/\sqrt{2}$.

indicate that cosp and sinp are eigenfunctions of the operator $\hat{L} + i\hat{\theta}/2\sigma^2$ with eigenvalue the phase point $L + i\theta/2\sigma^2$. The value of σ influences the operator and the functions favouring the θ variable when σ is small, or favouring the variable L for σ large, but, a value of $\sigma = 1/\sqrt{2}$ gives equal weight to both θ and L .

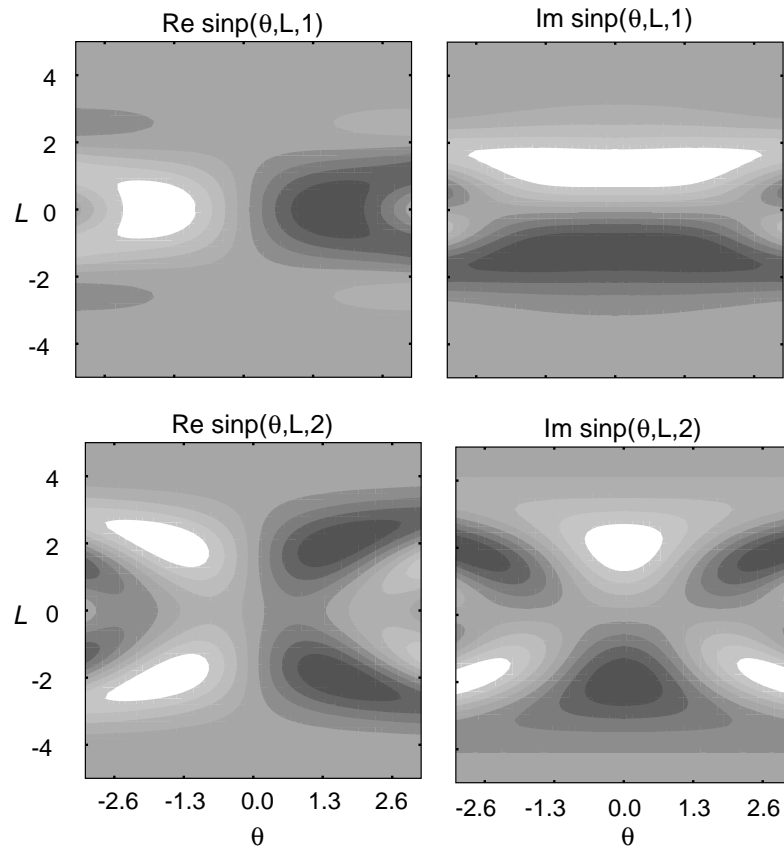


Figure 6. Density plots of the real and imaginary parts of $\text{sinp}(\theta, L, m)$ for $m = 1, 2$ and $\sigma = 1/\sqrt{2}$.

Other equalities are

$$\int d\theta e^{i\theta L/2} \text{sinp}(\theta, L, m) = -\frac{1}{m} e^{i\theta L/2} \text{cosp}(\theta, L, m) \quad (28)$$

$$\int d\theta e^{i\theta L/2} \text{cosp}(\theta, L, m) = \frac{1}{m} e^{i\theta L/2} \text{sinp}(\theta, L, m) \quad (29)$$

$$\left(\frac{L}{2} - i \frac{\partial}{\partial \theta}\right)^{-1} \text{sinp}(\theta, L, m) = -\frac{i}{m} \text{cosp}(\theta, L, m) \quad (30)$$

$$\left(\frac{L}{2} - i \frac{\partial}{\partial \theta}\right)^{-1} \text{cosp}(\theta, L, m) = \frac{i}{m} \text{sinp}(\theta, L, m) \quad (31)$$

where

$$\left(\frac{L}{2} - i \frac{\partial}{\partial \theta}\right)^{-1} = i e^{-i\theta L/2} \int d\theta e^{i\theta L/2} \quad (32)$$

and

$$\frac{1}{2\sigma\sqrt{2\pi}} \int_{-\pi}^{\pi} d\theta e^{iL(\theta - i2\sigma^2 L) + 2\sigma^2 m^2} \text{cosp}(\theta, L, m) \text{cosp}(\theta, L, n) = \delta_{m,n} \pi \quad (33)$$

$$\frac{1}{2\sigma\sqrt{2\pi}} \int_{-\pi}^{\pi} d\theta e^{iL(\theta-i2\sigma^2L)+2\sigma^2m^2} \text{sinp}(\theta, L, m) \text{sinp}(\theta, L, n) = \delta_{m,n} \pi \quad (34)$$

$$\frac{1}{2\sigma\sqrt{2\pi}} \int_{-\pi}^{\pi} d\theta e^{iL(\theta-i2\sigma^2L)+2\sigma^2m^2} \text{cosp}(\theta, L, m) \text{sinp}(\theta, L, n) = 0 \quad (35)$$

$$\int_{-\pi}^{\pi} d\theta \text{cosp}^*(\theta, L, m) \text{cosp}(\theta, L, n) = \delta_{m,n} \pi \sigma \sqrt{2\pi} [e^{-2\sigma^2(L-n)^2} + e^{-2\sigma^2(L+n)^2}] \quad (36)$$

$$\int_{-\pi}^{\pi} d\theta \text{cosp}^*(\theta, L, m) \text{sinp}(\theta, L, n) = -i\delta_{m,n} \pi \sigma \sqrt{2\pi} [e^{-2\sigma^2(L-n)^2} - e^{-2\sigma^2(L+n)^2}] \quad (37)$$

$$\int_{-\pi}^{\pi} d\theta \text{sinp}^*(\theta, L, m) \text{sinp}(\theta, L, n) = -\delta_{m,n} \pi \sigma \sqrt{2\pi} [e^{-2\sigma^2(L-n)^2} + e^{-2\sigma^2(L+n)^2}]. \quad (38)$$

From the last three equations, we see that the phase-space functions $\text{cosp}(\theta, L, m)$ and $\text{sinp}(\theta, L, m)$ are orthogonal, but $\text{cosp}^*(\theta, L, m)$ and $\text{sinp}(\theta, L, m)$ are not orthogonal, only when $e^{-2\sigma^2(L-n)^2} \approx e^{-2\sigma^2(L+n)^2}$, when $L \ll n$, $n \ll L$, $n = 0$, on the θ axis, i.e. $L = 0$, in the limit $\sigma \rightarrow 0$ or in the limit $\sigma \rightarrow \infty$.

Now, the solution to equation (13), which squared modulus has a period of π or 2π in θ , is written as the linear combination

$$w(\theta, L) = \sum_{n=0}^{\infty} [A_n \text{cosp}(\theta, L, n) + B_n \text{sinp}(\theta, L, n)] \quad (39)$$

where B_0 can be taken as zero. Upon substitution in the partial differential equation equation (13), one obtains

$$\begin{aligned} \sum_{m=-2}^{\infty} [(a-m^2)A_m - q(A_{m-2} + A_{m+2})] \text{cosp}(\theta, L, m) \\ + \sum_{m=-1}^{\infty} [(a-m^2)B_m - q(B_{m-2} + B_{m+2})] \text{sinp}(\theta, L, m) = 0 \end{aligned} \quad (40)$$

$$A_{-m}, B_{-m} = 0 \quad m > 0. \quad (41)$$

At this point, we note that the above relationship is the same as the one found in the solution of the usual Mathieu equation [12], with $\text{cosp}(\theta, L, m)$ and $\text{sinp}(\theta, L, m)$ replacing $\cos(m\theta)$ and $\sin(m\theta)$, respectively. With this in mind, we can take the results already developed for Mathieu functions. Equation (41) can be reduced to one of four simpler types,

$$\begin{aligned} w(\theta, L) &= \sum_{m=0}^{\infty} A_{2m+p} \text{cosp}(\theta, L, 2m+p) & p = 0 \text{ or } 1 \\ w(\theta, L) &= \sum_{m=0}^{\infty} B_{2m+p} \text{sinp}(\theta, L, 2m+p) & p = 0 \text{ or } 1 \end{aligned}$$

with recurrence relations $(a-m^2)A_m - q(A_{m-2} + A_{m+2}) = 0$ for even solutions ($aA_0 - qA_2 = 0$ for solutions with period π and $(a-1)A_1 - q(A_1 + A_3) = 0$ for solutions of period 2π) and $(a-m^2)B_m - q(B_{m-2} + B_{m+2}) = 0$ for odd solutions ($(a-4)B_2 - qB_4 = 0$ for solutions of period π and $(a-1)B_1 + q(B_1 - B_3) = 0$ for solutions of period 2π).

The characteristic values for a are

$$\begin{aligned} a_0(q) &= -\frac{q^2}{2} + \frac{7q^4}{128} - \frac{29q^6}{2304} + \frac{68687q^8}{18874368} + \dots \\ \left. \begin{aligned} a_1(-q) \\ b_1(q) \end{aligned} \right\} &= 1 - q - \frac{q^2}{8} + \frac{q^3}{64} - \frac{q^4}{1536} - \frac{11q^5}{36864} \end{aligned} \quad (42)$$

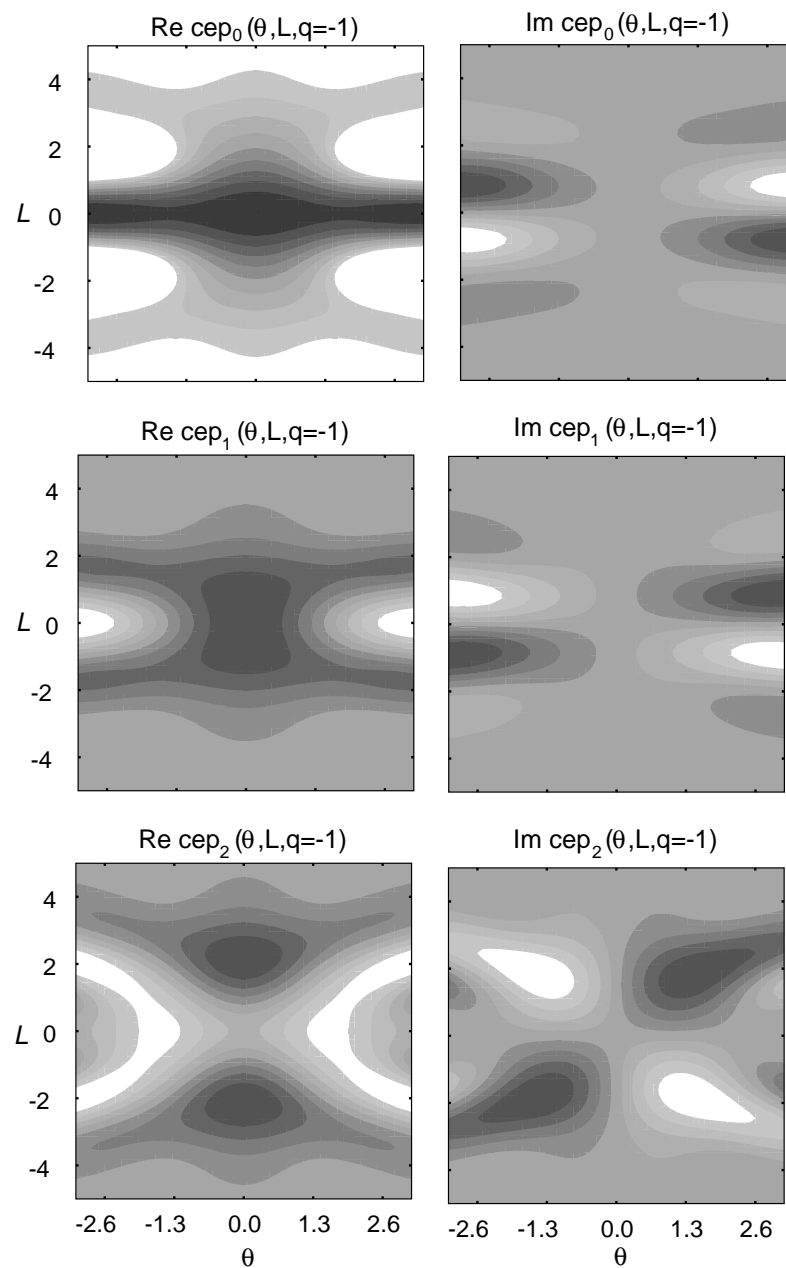


Figure 7. Density plots of the real and imaginary parts of $\text{cep}_n(\theta, L, q = -1)$ for $n = 0, 1, 2$ and $\sigma = 1/\sqrt{2}$.

$$+ \frac{49q^6}{589824} - \frac{55q^7}{9437184} - \frac{83q^8}{35389440} + \dots \quad (43)$$

$$b_2(q) = 4 - \frac{q^2}{12} + \frac{5q^4}{13824} - \frac{289q^6}{79626240} + \frac{21391q^8}{458647142400} + \dots \quad (44)$$

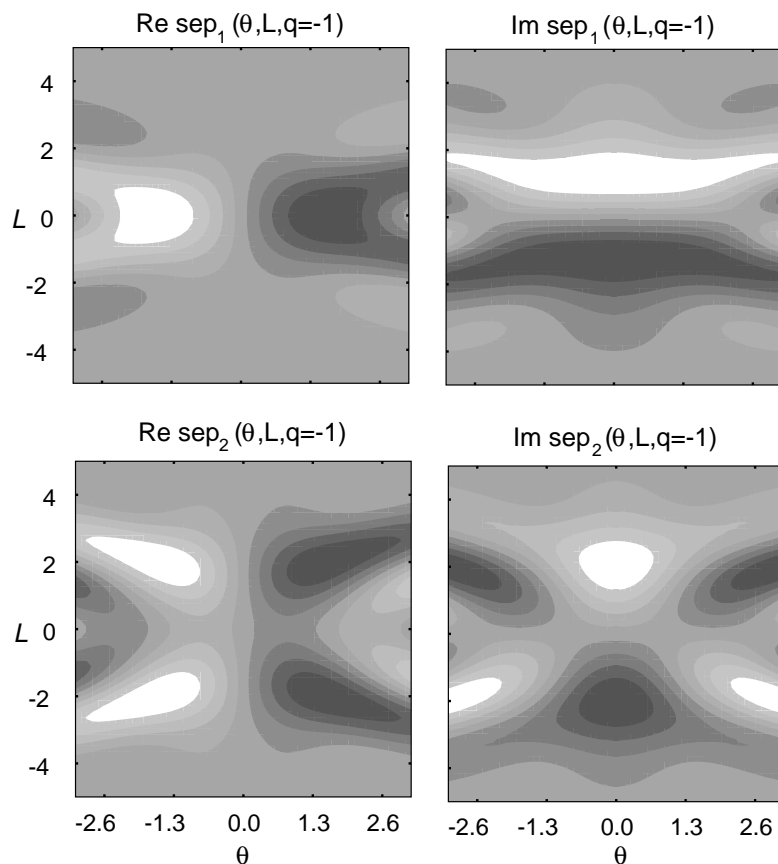


Figure 8. Density plots of the real and imaginary parts of $\text{sep}_n(\theta, L, q = -1)$ for $n = 1, 2$ and $\sigma = 1/\sqrt{2}$.

$$a_2(q) = 4 + \frac{5q^2}{12} - \frac{763q^4}{13824} + \frac{1002401q^6}{79626240} - \frac{1669068401q^8}{458647142400} + \dots \quad (45)$$

$$\left. \begin{array}{l} a_3(-q) \\ b_3(q) \end{array} \right\} = 9 + \frac{q^2}{16} - \frac{q^3}{64} + \frac{13q^4}{20480} + \frac{5q^5}{16384} - \frac{1961q^6}{23592960} + \frac{609q^7}{104857600} + \dots \quad (46)$$

with $a = a_r$ ($a = b_r$) associated with even (odd) periodic solutions. The corresponding functions are

$$\begin{aligned} \text{cep}_0(\theta, L, q) = & \frac{1}{\sqrt{2}} \left\{ \text{cosp}(\theta, L, 0) - \frac{q}{2} \text{cosp}(\theta, L, 2) \right. \\ & + q^2 \left[\frac{\text{cosp}(\theta, L, 4)}{32} - \frac{\text{cosp}(\theta, L, 0)}{16} \right] \\ & \left. - q^3 \left[\frac{\text{cosp}(\theta, L, 6)}{1152} - \frac{11 \text{cosp}(\theta, L, 2)}{128} \right] + \dots \right\} \end{aligned} \quad (47)$$

$$\begin{aligned} \text{cep}_1(\theta, L, q) = & \text{cosp}(\theta, L, 1) - \frac{q}{8} \text{cosp}(\theta, L, 3) \\ & + q^2 \left[\frac{\text{cosp}(\theta, L, 5)}{192} - \frac{\text{cosp}(\theta, L, 3)}{64} - \frac{\text{cosp}(\theta, L, 1)}{128} \right] \end{aligned}$$

$$-q^3 \left[\frac{\text{cosp}(\theta, L, 7)}{9216} - \frac{\text{cosp}(\theta, L, 5)}{1152} - \frac{\text{cosp}(\theta, L, 3)}{3072} + \frac{\text{cosp}(\theta, L, 1)}{512} \right] + \dots \quad (48)$$

$$\begin{aligned} \text{sep}_1(\theta, L, q) &= \text{sinp}(\theta, L, 1) - \frac{q}{8} \text{sinp}(\theta, L, 3) \\ &+ q^2 \left[\frac{\text{sinp}(\theta, L, 5)}{192} + \frac{\text{sinp}(\theta, L, 3)}{64} - \frac{\text{sinp}(\theta, L, 1)}{128} \right] \\ &- q^3 \left[\frac{\text{sinp}(\theta, L, 7)}{9216} + \frac{\text{sinp}(\theta, L, 5)}{1152} - \frac{\text{sinp}(\theta, L, 3)}{3072} - \frac{\text{sinp}(\theta, L, 1)}{512} \right] \\ &+ \dots \end{aligned} \quad (49)$$

$$\begin{aligned} \text{cep}_2(\theta, L, q) &= \text{cosp}(\theta, L, 2) - q \left[\frac{\text{cosp}(\theta, L, 4)}{12} - \frac{\text{cosp}(\theta, L, 0)}{4} \right] \\ &+ q^2 \left[\frac{\text{cosp}(\theta, L, 6)}{384} - \frac{19\text{cosp}(\theta, L, 2)}{288} \right] + \dots \end{aligned} \quad (50)$$

$$\begin{aligned} \text{sep}_2(\theta, L, q) &= \text{sinp}(\theta, L, 2) - q \frac{\text{sinp}(\theta, L, 4)}{12} + q^2 \left[\frac{\text{sinp}(\theta, L, 6)}{384} - \frac{\text{sinp}(\theta, L, 2)}{288} \right] \\ &+ \dots \end{aligned} \quad (51)$$

For higher-order solutions, we can use

$$\begin{aligned} \text{cep}_v(\theta, L, q) &= \text{cosp}(\theta, L, v) - \frac{q}{4} \left[\frac{\text{cosp}(\theta, L, v+2)}{(v+1)} - \frac{\text{cosp}(\theta, L, v-2)}{(v-1)} \right] \\ &+ \frac{q^2}{32} \left[\frac{\text{cosp}(\theta, L, v+4)}{(v+1)(v+2)} + \frac{\text{cosp}(\theta, L, v-4)}{(v-1)(v-2)} \right] \\ &- \frac{q^3}{128} \left[\frac{(v^2+4v+7)\text{cosp}(\theta, L, v+2)}{(v-1)(v+1)^3(v+2)} - \frac{(v^2-4v+7)\text{cosp}(\theta, L, v-2)}{(v+1)(v-1)^3(v-2)} \right] \\ &+ \frac{\text{cosp}(\theta, L, v+6)}{3(v+1)(v+2)(v+3)} - \frac{\text{cosp}(\theta, L, v-6)}{3(v-1)(v-2)(v-3)} + \dots \end{aligned} \quad (52)$$

$$\begin{aligned} \text{sep}_v(\theta, L, q) &= \text{sinp}(\theta, L, v) - \frac{q}{4} \left[\frac{\text{sinp}(\theta, L, v+2)}{(v+1)} - \frac{\text{sinp}(\theta, L, v-2)}{(v-1)} \right] \\ &+ \frac{q^2}{32} \left[\frac{\text{sinp}(\theta, L, v+4)}{(v+1)(v+2)} + \frac{\text{sinp}(\theta, L, v-4)}{(v-1)(v-2)} \right] - \dots \end{aligned} \quad (53)$$

where

$$a = v^2 + \frac{q^2}{2(v^2-1)} + \frac{(5v^2+7)}{32(v^2-1)^3(v^2-4)}q^4 + \frac{9v^4+58v^2+29}{64(v^2-1)^5(v^2-4)(v^2-9)}q^6 + \dots \quad (54)$$

and $q^2/2(v^2-1) \ll v^2$, $v = m + p/s$, m a positive integer. The squared magnitude of these functions have period $2\pi s$ or πs in θ accordingly as p is odd or even, $s \geq 2$. Density plots of some of these functions can be found in figures 7 and 8. In the limit of $\sigma \rightarrow 0$, these functions approach the usual one-variable Mathieu functions, and for $\sigma \rightarrow \infty$, they approach the Fourier transform of Mathieu functions, a collection of delta functions centred at $L \pm m$.

These functions are also eigenfunctions of the operator $\hat{L} + i\hat{\theta}/2\sigma^2$ with eigenvalue as the phase point $L + i\theta/2\sigma^2$,

$$\left[\left(\frac{L}{2} - i \frac{\partial}{\partial \theta} \right) + \frac{i}{2\sigma^2} \left(\frac{\theta}{2} + i \frac{\partial}{\partial L} \right) \right] \text{cep}_i(\theta, L, q) = \left(L + \frac{i\theta}{2\sigma^2} \right) \text{cep}_i(\theta, L, q) \quad (55)$$

$$\left[\left(\frac{L}{2} - i \frac{\partial}{\partial \theta} \right) + \frac{i}{2\sigma^2} \left(\frac{\theta}{2} + i \frac{\partial}{\partial L} \right) \right] \text{sep}_i(\theta, L, q) = \left(L + \frac{i\theta}{2\sigma^2} \right) \text{sep}_i(\theta, L, q). \quad (56)$$

We can see that a value of $\sigma = 1/\sqrt{2}$ gives equal weight to both θ and L .

As for $\text{cosp}(\theta, L, m)$ and $\text{sinp}(\theta, L, m)$ the functions $\text{cep}_n(\theta, L, q)$ and $\text{sep}_n(\theta, L, q)$ are orthogonal (see equations (34)–(38)), but $\text{cep}_n^*(\theta, L, q)$ and $\text{sep}_n(\theta, L, q)$ are orthogonal only when $0 \ll L$, on the θ axis, i.e. $L = 0$, in the limit $\sigma \rightarrow 0$, which corresponds to the coordinate space, or in the limit $\sigma \rightarrow \infty$, which corresponds to the momentum representation.

References

- [1] Husimi K 1940 *Proc. Phys. Math. Soc. Japan* **22** 264
- [2] Klauder J R and Skagerstam B S 1985 *Coherent States* (Singapore: World Scientific)
- [3] Perelomov A 1986 *Generalized Coherent States and Their Applications: Texts and Monographs in Physics* (Berlin: Springer)
- [4] Glauber R J 1963 *Phys. Rev.* **130** 2529
Glauber R J 1963 *Phys. Rev.* **131** 2766
- [5] Harriman J E 1994 *J. Chem. Phys.* **100** 3651
- [6] Włodarz J J 1994 *J. Chem. Phys.* **100** 7476
- [7] Skodje R T, Rohts H W and VanBuskirk J 1989 *Phys. Rev. A* **40** 2894
- [8] Torres-Vega Go and Frederick J H 1991 *Phys. Rev.* **67** 2601
Torres-Vega Go and Frederick J H 1990 *J. Chem. Phys.* **93** 8862
Torres-Vega Go and Frederick J H 1993 *J. Chem. Phys.* **98** 3103
- [9] Torres-Vega Go and Morales-Guzmán J D 1994 *J. Chem. Phys.* **101** 5847
- [10] Torres-Vega Go 1993 *J. Chem. Phys.* **98** 7040
Torres-Vega Go 1993 *J. Chem. Phys.* **99** 1824
- [11] Møller K B and Jørgensen T G 1997 *J. Chem. Phys.* **106** 7228
- [12] McLachlan N W 1964 *Theory and Application of Mathieu Functions* (New York: Dover)
Staff of the Bateman Manuscript Project 1955 *Higher Transcendental Functions* (New York: McGraw-Hill)
Whittaker E T and Watson G N 1963 *A Course of Modern Analysis* (Cambridge: Cambridge University Press)
Wang Z X and Guo D R 1989 *Special Functions* (Singapore: World Scientific)
Erdélyi, Magnus, Oberhettinger and Tricomi 1953 *Higher Transcendental Functions* (New York: McGraw-Hill)
Abramowitz M and Stegun I A 1972 *Handbook of Mathematical Functions* (New York: Dover)
- [13] Condon E U 1928 *Phys. Rev.* **31** 891
Pradhan T and Khare A V 1973 *Am. J. Phys.* **41** 59
Kesarwani R N and Varxhni Y P 1982 *J. Math. Phys.* **23** 92
Aquino N and Piña E 1993 *Rev. Mex. Fis.* **39** 945
- [14] Torres-Vega Go, Møller K and Zúñiga-Segundo A *Phys. Rev. A* in press